



Semi-mechanistic Modeling of Hypoxanthine, Xanthine, and Uric Acid Metabolism in Asphyxiated Neonates

Wan-Yu Chu¹ · Karel Allegaert^{2,3} · Thomas P. C. Dorlo¹ · Alwin D. R. Huitema^{1,4,5} on behalf of the ALBINO Study Group

Accepted: 24 July 2022 / Published online: 30 August 2022
© The Author(s) 2022

Abstract

Background and Objective Previously, we developed a pharmacokinetic-pharmacodynamic model of allopurinol, oxypurinol, and biomarkers, hypoxanthine, xanthine, and uric acid, in neonates with hypoxic-ischemic encephalopathy, in which high initial biomarker levels were observed suggesting an impact of hypoxia. However, the full pharmacodynamics could not be elucidated in our previous study. The current study included additional data from the ALBINO study (NCT03162653) placebo group, aiming to characterize the dynamics of hypoxanthine, xanthine, and uric acid in neonates with hypoxic-ischemic encephalopathy.

Methods Neonates from the ALBINO study who received allopurinol or placebo mannitol were included. An extended population pharmacokinetic-pharmacodynamic model was developed based on the mechanism of purine metabolism, where synthesis, salvage, and degradation via xanthine oxidoreductase pathways were described. The initial level of the biomarkers was a combination of endogenous turnover and high disease-related amounts. Model development was accomplished by nonlinear mixed-effects modeling (NONMEM[®], version 7.5).

Results In total, 20 neonates treated with allopurinol and 17 neonates treated with mannitol were included in this analysis. Endogenous synthesis of the biomarkers reduced with 0.43% per hour because of precursor exhaustion. Hypoxanthine was readily salvaged or degraded to xanthine with rate constants of 0.5 1/h (95% confidence interval 0.33–0.77) and 0.2 1/h (95% confidence interval 0.09–0.31), respectively. A greater salvage was found in the allopurinol treatment group consistent with its mechanism of action. High hypoxia-induced initial levels of biomarkers were quantified, and were 1.2-fold to 2.9-fold higher in neonates with moderate-to-severe hypoxic-ischemic encephalopathy compared with those with mild hypoxic-ischemic encephalopathy. Half-maximal xanthine oxidoreductase inhibition was achieved with a combined allopurinol and oxypurinol concentration of 0.68 mg/L (95% confidence interval 0.48–0.92), suggesting full xanthine oxidoreductase inhibition during the period studied.

Conclusions This extended pharmacokinetic-pharmacodynamic model provided an adequate description of the complex hypoxanthine, xanthine, and uric acid metabolism in neonates with hypoxic-ischemic encephalopathy, suggesting a positive allopurinol effect on these biomarkers. The impact of hypoxia on their dynamics was characterized, underlining higher hypoxia-related initial exposure with a more severe hypoxic-ischemic encephalopathy status.

1 Introduction

Perinatal asphyxia due to a hypoxic-ischemic event is a major cause of mortality and neurodevelopmental disability in neonates. One profound complication of perinatal asphyxia is global cerebral injury, known as hypoxic-ischemic

encephalopathy (HIE) [1]. The pathophysiology of HIE, as a consequence of energy failure, involves a series of adaptations in purine metabolism, including interconversions of upstream purine nucleotides and nucleosides and their degradations to hypoxanthine, xanthine, and eventually to uric acid [2].

In hypoxia, the production of adenosine triphosphate is hindered by a lack of oxygen, which accelerates the breakdown of adenosine monophosphate (AMP) to maintain energy levels [3]. Adenosine monophosphate enters the purine degradation pathway forming purine nucleotides and nucleosides, leading to formation of the purine base hypoxanthine, which oxidizes to xanthine and eventually

The members of the ALBINO Study Group are listed in Acknowledgements.

✉ Alwin D. R. Huitema
a.huitema@nki.nl

Extended author information available on the last page of the article

Key Points

Positive pharmacological effect of allopurinol in neonates with hypoxic-ischemic encephalopathy was supported by sufficient xanthine oxidoreductase inhibition and a high fraction of hypoxanthine salvage.

The impact of hypoxia on hypoxanthine, xanthine, and uric acid dynamics was characterized in the model. Synthesis of the hypoxanthine and xanthine reduced because of precursor exhaustion.

Higher hypoxia-related initial hypoxanthine and xanthine values with a more severe hypoxic-ischemic encephalopathy status was found.

to uric acid via xanthine oxidoreductase (XOR) [2]. Under normal conditions, the majority of hypoxanthine is reutilized through the salvage pathway [4, 5]. While in hypoxia, the rate of salvage and degradation decreases because of energy deficiency, which results in hypoxanthine accumulation [6]. During the reoxygenation–reperfusion stage following resuscitation, hypoxanthine substantially oxidizes to xanthine and uric acid. Of note, in the presence of a high oxygen supplementation, specific proteases prompt the switch from xanthine dehydrogenase to xanthine oxidase, which uses oxygen as a substrate causing the surge of free radicals that will cause brain injury in neonates [7].

Despite therapeutic hypothermia (TH) as a standard treatment for moderate-to-severe HIE, the improvement in the neurological outcome of neonates with HIE remains unsatisfactory [8]. Allopurinol, a XOR inhibitor that reduces the production of free radicals, has been introduced as a potential neuroprotective intervention in HIE [9]. The ALBINO study, a blinded randomized placebo-controlled parallel-group trial, is currently investigating the effect of postnatal allopurinol treatment, along with TH and standard of care, on the incidence of death and severe neurodevelopmental impairment in neonates with HIE [10].

Hypoxanthine, xanthine, and uric acid are downstream products of purine metabolism, and their potential roles as biomarkers have been underlined [2]. Hypoxanthine and uric acid, of which the former is a direct product of the hypoxic-ischemic event, and the latter is the end metabolite of purine metabolism, have been suggested as biochemical markers informing the stage of HIE [6, 12–15]. In addition, as substrates of XOR, hypoxanthine, xanthine, and uric acid have been applied as pharmacodynamic (PD) markers for several XOR inhibitors [11]. However, the pharmacokinetic (PK)-PD effects and the

pathophysiological effects of hypoxia on hypoxanthine, xanthine, and uric acid dynamics have not been thoroughly studied.

Previously, we described the effect of allopurinol and oxypurinol on hypoxanthine, xanthine, and uric acid in neonates with HIE using a population PK-PD approach [16]. In that study, high initial hypoxanthine, xanthine, and uric acid levels were observed, possibly as a result of hypoxia [16]. However, the full pathophysiological dynamics of hypoxanthine, xanthine, and uric acid due to natural recovery could not be elucidated in our previous study, as the model was based on data from asphyxiated neonates receiving allopurinol intervention only. In the current study, additional hypoxanthine, xanthine, and uric acid data from the ALBINO placebo group, receiving mannitol instead of allopurinol, was included [10]. To comprehend the possible interpretation of hypoxanthine, xanthine, and uric acid levels in neonates with HIE and to delineate the effect of allopurinol treatment, this study aimed to further characterize the metabolism of purine bases hypoxanthine, xanthine, and uric acid in neonates with HIE using a semi-mechanistic population modeling approach.

2 Methods

2.1 Clinical Trial and Population

The ALBINO study is an ongoing, double-blind, placebo-controlled, randomized phase III trial [10]. Neonates receive either intravenous allopurinol or the placebo mannitol. As a standard of care, neonates classified as moderate-to-severe HIE undergo TH. The PK-PD sub-study was conducted in four centers (University Medical Centre Utrecht and Amsterdam UMC location VUMC in The Netherlands, and University Hospital Tuebingen and Cnopf Children's Hospital Nuremberg in Germany) involved in the ALBINO study and was approved by all relevant national and institutional medical ethics committees (NL57237.041.16; EudraCT 2016-000222-19).

In this analysis, neonates from the ALBINO PK-PD sub-study receiving allopurinol (verum) and mannitol (placebo) were included. An initial dose of 20 mg/kg of allopurinol or placebo was given within 45 minutes after birth, following a second dose of 10 mg/kg in TH-treated neonates with a 12-h interval. Allopurinol and oxypurinol plasma concentrations were measured in patients allocated to the verum group, and mannitol plasma concentrations were measured in patients allocated to the placebo group. Hypoxanthine, xanthine, and uric acid plasma levels were measured in both studied groups. The blood sampling schedule and bioanalysis method were described in previously published

studies related to the ALBINO study [16, 17]. Data sharing and flow hereby secured the blinding process throughout this analysis. To further ensure this, we have reported by median and interquartile range in the event of a non-normal distribution.

2.2 Model Development

This semi-mechanistic model is an extension of our previous model describing the pharmacokinetics/pharmacodynamics of allopurinol, oxypurinol, hypoxanthine, xanthine, and uric acid in neonates with HIE who received allopurinol. In our previous study, the pharmacokinetics of allopurinol and oxypurinol was described by two sequential one-compartment models with an autoinhibition effect on allopurinol metabolism by oxypurinol. The pharmacodynamics was described by a turnover model of hypoxanthine to xanthine and subsequently to uric acid assuming full conversions between each compound. As this model was established only based on data from allopurinol-treated neonates, it was not possible to distinguish between treatment and disease-related effects. As a starting point, the previously developed model was fitted to the updated dataset. Subsequently, disease-related mechanisms were included in the model.

In the refined model, the framework of our previous PK model was used and the PD model was expanded based on the mechanism of purine metabolism [2, 16]. In addition to the degradation of hypoxanthine to xanthine and xanthine to uric acid via XOR, the salvage pathway was included as an additional clearance of hypoxanthine. Furthermore, the synthesis of hypoxanthine and xanthine from the *de novo* synthesis pathway and potential AMP breakdown were included.

As defined in our previous model, the effect of allopurinol and oxypurinol concentrations on XOR inhibition (EFF) was described by an E_{\max} function with a fixed maximal effect of 1 assuming full inhibition at high concentrations (Eq. 1):

$$\text{EFF} = \frac{E_{\max} * (\text{Concentration}_{\text{allopurinol}} + \text{Concentration}_{\text{oxypurinol}})}{\text{IC}_{50} + (\text{Concentration}_{\text{allopurinol}} + \text{Concentration}_{\text{oxypurinol}})} \quad (1)$$

The initial levels of hypoxanthine, xanthine, and uric acid were a combination of endogenous turnover (EBASE_n) and high initial hypoxia-related amounts (Init_{nD}) (Eq. 2):

$$A_n(0) = \text{EBASE}_n + \text{Init}_{nD} \quad (2)$$

The mass balances describing the synthesis of hypoxanthine and xanthine, the degradation of hypoxanthine to xanthine and to uric acid, the salvage of hypoxanthine, and the effect of allopurinol and oxypurinol on XOR inhibition are summarized in Eqs. 3–5:

$$\frac{dA(\text{hypoxanthine})}{dt} = \frac{dA(4)}{dt} = k_{in4} - k_{45} * A(4) * \text{EFF} - k_{40} * A(4), \quad (3)$$

$$\frac{dA(\text{xanthine})}{dt} = \frac{dA(5)}{dt} = k_{in5} + k_{45} * A(4) * \text{EFF} - k_{56} * A(5) * \text{EFF}, \quad (4)$$

$$\frac{dA(\text{uric acid})}{dt} = \frac{dA(6)}{dt} = k_{56} * A(5) * \text{EFF} - k_{60} * A(6). \quad (5)$$

In which k_{in4} , k_{45} , and k_{40} are the rate of hypoxanthine synthesis, degradation to xanthine, and salvage, respectively. k_{in5} and k_{56} are the rate of xanthine synthesis and degradation to uric acid, respectively. k_{60} is the elimination rate of uric acid. EFF is the effect of allopurinol and oxypurinol on XOR inhibition.

The modeling process was performed using a nonlinear mixed-effects modeling program (NONMEM, version 7.5; Icon Development Solutions, Whitesboro, NY, USA) aided by Perl-speaks-NONMEM (PsN, version 4.9) [18, 19]. Model fit was computed using the first-order conditional estimation with interaction method with interaction between interindividual variability (IIV) and residual error components. Individual Bayesian estimates were obtained using the POSTHOC option. Interindividual variability in the parameters was estimated using an exponential model. Residual variability was estimated for all substrates using a proportional error model. Pirana (version 2.9.9) was used for run management [20]. R (version 4.0) was used for the graphical model evaluation.

2.3 Covariate Analysis

Factors reflecting disease status, including TH, Thompson score (T-score), lactate dehydrogenase (LDH), alanine aminotransferase (ALT) were plotted against individual variability in disease-related initial hypoxanthine, xanthine, and uric acid levels. The T-score is clinically indicated for HIE

severity classification and for assessing the need for TH [21]. In the ALBINO study, implementing TH was guided by a T-score defined at 2–6 hours after birth together with amplitude-integrated electroencephalography monitoring. Lactate dehydrogenase and ALT are parameters characterizing cell necrosis and tissue damage in neonates [22, 23]. As TH might alter systematic perfusion, the influence of TH for variability in rate-specific parameters were evaluated [24]. Therapeutic hypothermia was evaluated as a binary covariate, and LDH and ALT were evaluated as continuous

covariates. The T-score was tested as a continuous covariate and a binary covariate using a cut-off value of 8, as a T-score above 8 irrespective of amplitude-integrated electroencephalography was defined as moderate-to-severe HIE in the ALBINO study [10]. Covariate-parameter relationships that showed a visual trend in graphical assessment were introduced in the base model and tested for significance.

2.4 Model Evaluation

Model adequacy was evaluated using statistical and graphical methods as well as physiological plausibility. The objective function value (OFV), equal to minus 2 times the log likelihood, was used as an indicator of goodness of fit. When comparing the goodness of fit between nested models, a decrease in OFV of > 3.84 corresponding to a p -value of < 0.05 was considered statistically significant, which follows a chi-square distribution with an additional one degree of freedom. Goodness-of-fit plots and a visual predictive check were performed for the model evaluation [25]. Parameter precision and the 95% confidence interval were assessed with sampling importance resampling [26].

3 Results

3.1 Patient Characteristics

In total, 20 neonates who received allopurinol and 17 neonates who received mannitol were included, and 97 allopurinol, 97 oxypurinol, 165 hypoxanthine, 159 xanthine, and 171 uric acid observations were analyzed, respectively. The

observed concentration–time data of hypoxanthine, xanthine, and uric acid are shown in Fig. 1. Overall, 26 neonates were classified as moderate-to-severe HIE and underwent TH treatment. Details on the dataset and patient characteristics are summarized in Table 1.

3.2 Model Development

The model described by Eqs. 1–5 was applied to the data but overpredicted the endogenous baseline of hypoxanthine and xanthine. As can be observed in Fig. 1, steady-state concentrations of hypoxanthine and xanthine were not reached within the observation period, while the model predicted the steady state being reached. Hypoxanthine and xanthine are products of purine nucleotides and nucleosides, which are highly dynamic under a hypoxic status owing to a substantial AMP breakdown [27]. In hypoxic animals, a dramatic increase in purine precursors (including purine nucleotides such as inosine monophosphate, guanosine monophosphate, and purine nucleosides such as inosine and guanosine) following a rapid decline has been identified [28, 29]. Therefore, the influence of dynamic purine precursors on the synthesis of hypoxanthine and xanthine was investigated.

An empirical compartment was added to the model, representing pooled precursors in purine metabolism. As no measurement was available for the precursors, the initial amount in compartment was assumed to be 1, and all relevant rate process were therefore, relative to the rate at time 0. At equilibrium, the turnover of precursors compartment composed of a zero-order synthesis rate constant (k_{in3}) and a first-order elimination rate constant (k_{30}) as described in Eq. 6.

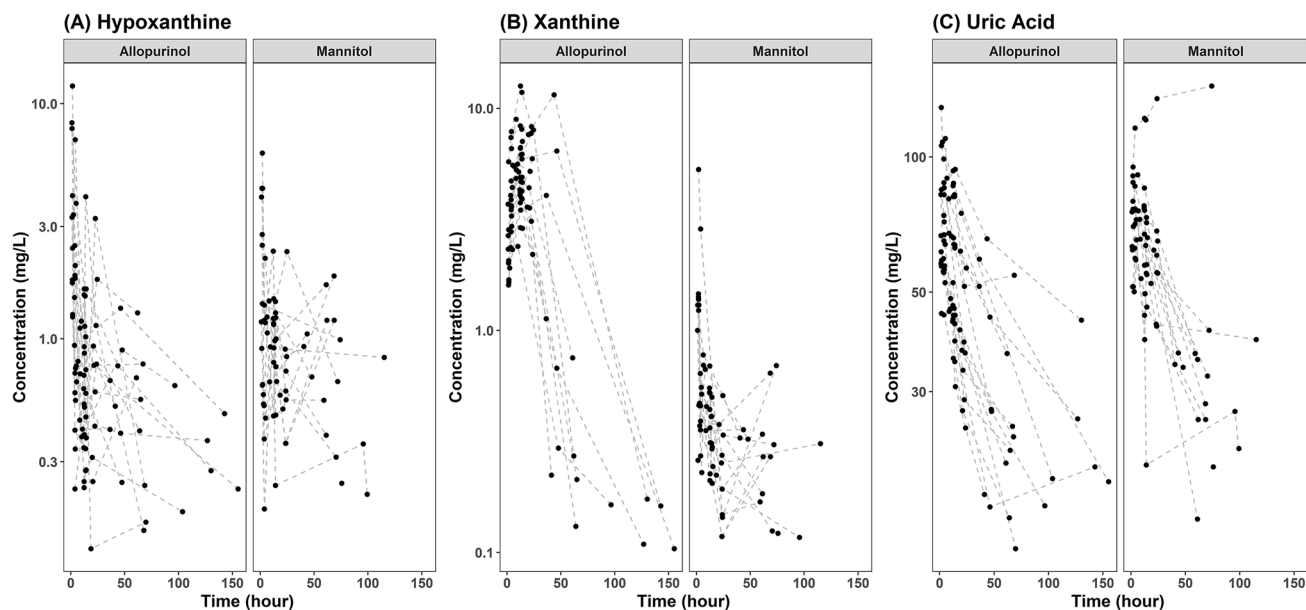


Fig. 1 Observed concentration–time profiles

Table 1 Data and patient demographics

	Allopurinol group (N = 20)	Mannitol group (N = 17)	Overall (N = 37)
<i>Observation, n</i>			
Allopurinol	97	–	97
Oxypurinol	97	–	97
Hypoxanthine	92	73	165
Xanthine	86	73	159
Uric acid	94	77	171
<i>Birthweight, g</i>			
Mean (SD)	3490 (582)	3420 (455)	3460 (521)
<i>Height, cm</i>			
Mean (SD)	50.8 (4.09)	51.7 (3.20)	51.2 (3.67)
<i>Sex, n (%)</i>			
Female	11 (55.0%)	12 (70.6%)	23 (62.2%)
Male	9 (45.0%)	5 (29.4%)	14 (37.8%)
<i>Gestational age, weeks</i>			
Mean (SD)	39.2 (1.79)	39.5 (1.50)	39.3 (1.65)
<i>Hypothermia, n (%)</i>			
Yes (moderate-to-severe HIE)	13 (65.0%)	13 (76.5%)	26 (70.3%)
No (mild HIE)	7 (35.0%)	4 (23.5%)	11 (29.7%)
<i>Thompson score at 2–6 hours</i>			
Median [IQR]	6.50 [5.00–10.0]	10.5 [5.00–13.8]	7.50 [5.00–11.0]
<i>Lactate dehydrogenase at 24 hours, U/L</i>			
Median [IQR]	1130 [718–1890]	912 [539–1210]	996 [705–1510]
<i>Alanine aminotransferase at 24 hours, U/L</i>			
Median [IQR]	48.0 [24.3–83.5]	29.0 [17.5–45.5]	37.0 [19.0–62.8]

HIE hypoxic-ischemic encephalopathy, IQR interquartile range, SD standard deviation

$$\frac{dA(\text{precursors})}{dt} = \frac{dA(3)}{dt} = k_{in3} - k_{30} * A(3). \quad (6)$$

This equation could be further simplified given that the initial amount of precursors is dominated by the hypoxic state, and is extensively higher than the physiological steady-state ($\frac{k_{in3}}{k_{30}}$) [30]. Therefore, k_{in3} was omitted resulting in a net first-order decline in total amount over time during the observation period as shown in Eq. 7:

$$\frac{dA(\text{precursors})}{dt} = \frac{dA(3)}{dt} = -k_{30} * A(3). \quad (7)$$

To describe the impact of upstream precursor exhaustion on downstream hypoxanthine and xanthine synthesis, k_{in4} and k_{in5} were further regulated by the amount in the pooled precursors compartment [A(3)] as described in Eqs. 8–9:

$$\begin{aligned} \frac{dA(\text{hypoxanthine})}{dt} &= \frac{dA(4)}{dt} \\ &= k_{in4} * A(3) - k_{45} * A(4) * \text{EFF} - k_{40} * A(4), \end{aligned} \quad (8)$$

$$\begin{aligned} \frac{dA(\text{xanthine})}{dt} &= \frac{dA(5)}{dt} \\ &= k_{in5} * A(3) + k_{45} * A(4) * \text{EFF} - k_{56} * A(5) * \text{EFF}. \end{aligned} \quad (9)$$

Incorporating the precursors effect in the model improved the description of hypoxanthine and xanthine endogenous turnover. Estimated k_{30} was 0.0043 1/h, implying that the production of hypoxanthine and xanthine was reduced by 0.43% per hour because of precursor exhaustion after hypoxia.

The final structure of the model is depicted in Fig. 2. All PK and PD parameters were estimated simultaneously, and the final estimates with corresponding 95% confidence intervals are shown in Table 2. In the final model, PK parameters were comparable to our previous estimations. Allopurinol clearance and volume of distribution was 0.74 L/h and 2.8 L, respectively. Oxypurinol clearance and volume of distribution relative to a formation fraction were 0.3 L/h and 10.39 L, respectively. The auto-inhibition of

allopurinol-oxypurinol metabolism achieved a half-maximal effect under an oxypurinol concentration of 2.96 mg/L.

In the final PD model, the estimated baseline production of hypoxanthine (k_{in4}) and xanthine (k_{in5}) was 0.49 mg/L*h and 0.66 mg/L*h, respectively. Hypoxanthine was readily salvaged or degraded to xanthine with rate constants of 0.5 1/h and 0.2 1/h, respectively. In the allopurinol and the mannitol group, the salvage pathway accounted for 75% and 68% of total hypoxanthine clearance, respectively. High disease-related initial level of hypoxanthine ($Init_{4D}$), xanthine ($Init_{5D}$), and uric acid ($Init_{6D}$) was estimated (0.45 mg/L, 0.59 mg/L and 37.98 mg/L, respectively). The effect of drug treatment on XOR inhibition was described, where the half-maximal XOR inhibition (IC_{50}) was achieved with a combined allopurinol and oxypurinol concentration of 0.68 mg/L. This IC_{50} was below all observed concentrations within 72 hours post-dose.

3.3 Covariate Analysis and Correlations

High IIVs in the disease-related initial level of hypoxanthine ($Init_{4D}$), xanthine ($Init_{5D}$), and uric acid ($Init_{6D}$) were

found. A trend towards higher disease-related hypoxanthine, xanthine, and uric acid estimates with a more severe HIE status, indicated by T-score or TH, was seen in the graphical analysis (Fig. 1 of the ESM). Furthermore, patients with very high LDH (> 2500 U/L) and ALT (> 100 U/L) values, suggesting more serious organ damage, demonstrated higher disease-related hypoxanthine and xanthine values (Fig. 2 of the ESM). The T-score and TH were therefore tested as binary covariates on $Init_{4D}$, $Init_{5D}$, and $Init_{6D}$.

Adding TH as a binary covariate on $Init_{4D}$ and $Init_{5D}$ significantly improved the model goodness of fit with a OFV drop of 5.05 units, and reduced IIV in $Init_{4D}$ and $Init_{5D}$ by more than 35%. Neonates with moderate-to-severe HIE (thus treated with TH) had 2.9-fold and 1.2-fold higher $Init_{4D}$ and $Init_{5D}$ than neonates with mild HIE, respectively. $Init_{6D}$ was not significantly different between the TH and non-TH group. A correlation of 1 between IIV in $Init_{4D}$ and $Init_{5D}$ was estimated, which resulted in a 20-unit drop in OFV. To reduce model complexity, the same ETA distribution was assigned for IIV in $Init_{4D}$ and in $Init_{5D}$ with a scaling factor of 0.66 estimated for the latter. The correlation between either IIV $Init_{4D}$ or IIV $Init_{5D}$ and IIV $Init_{6D}$ was below 0.35;

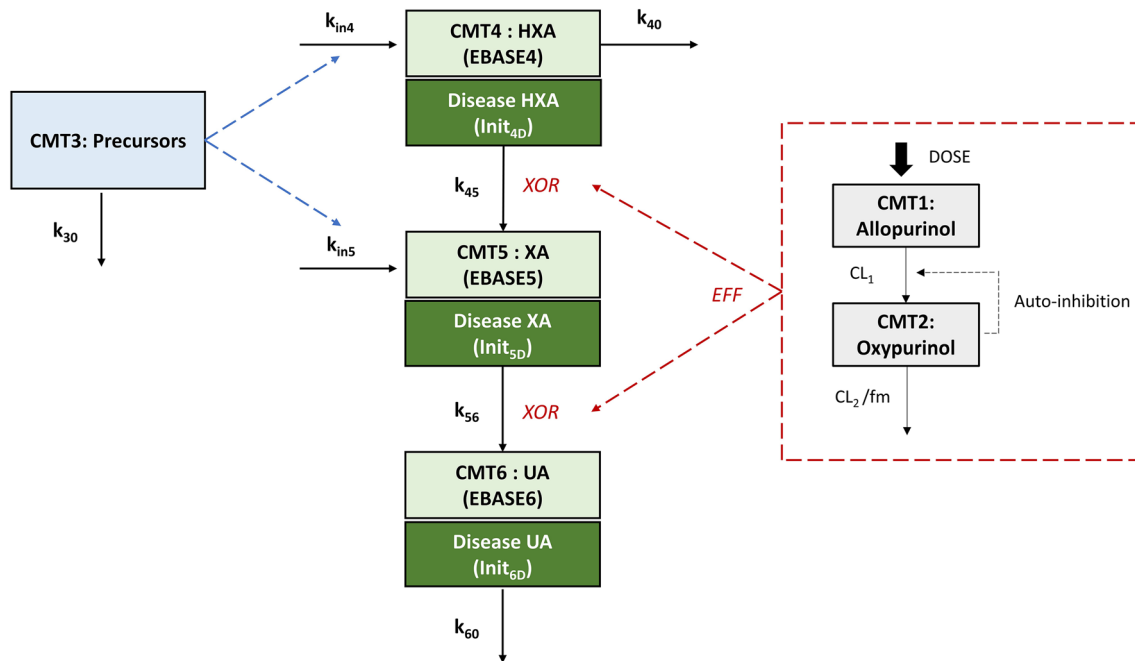


Fig. 2 Final model structure. Gray shades, pharmacokinetic model of allopurinol and oxypurinol with an autoinhibition effect on allopurinol metabolism by oxypurinol. Red broken line, xanthine oxidase inhibition by allopurinol and oxypurinol (EFF). Blue broken line, the impact of purine nucleotides and nucleoside level on the generation of hypoxanthine and xanthine. *EBASE4* hypoxanthine baseline value, *EBASE5* xanthine baseline value, *EBASE6* uric acid baseline value,

Init4D disease-related hypoxanthine initial value, *Init5D* disease-related xanthine initial value, *Init6D* disease-related uric acid initial value, k_{30} precursors clearance, k_{40} hypoxanthine salvage clearance, k_{45} hypoxanthine to xanthine clearance, k_{56} xanthine to uric acid clearance, k_{60} uric acid clearance, kin_4 hypoxanthine synthesis rate, kin_5 xanthine synthesis rate, HXA hypoxanthine, XA xanthine, UA uric acid, XOR xanthine oxidoreductase.

Table 2 Final parameter estimates

	Parameter	Unit	Estimate	95% CI	IIV (%)	95% CI
<i>PK model</i>						
Allopurinol (CMT1)	CL1	L/h	0.74	0.52–1.07	61	46–76
	V1	L	2.8	2.38–3.28	21	13–27
Oxypurinol (CMT2)	CL2/fm	L/h	0.3	0.23–0.38	42	31–55
	V2/fm	L	10.39	8.83–12.42	31	22–40
Auto-inhibition	IC _{50 auto}	mg/L	2.96	1.77–4.61	–	–
<i>PD model</i>						
XO inhibition (EFF)	IC ₅₀	mg/L	0.68	0.48–0.92	–	–
Precursors (CMT3)	k ₃₀	1/h	0.0043	0.0025–0.0061	–	–
Hypoxanthine (CMT4)	k _{in4}	mg/L* ^a h	0.49	0.32–0.74	–	–
	E _{BASE} (4) ^a	mg/L	0.7 ^a	–	–	–
	Init _{4D}	mg/L	0.45	0.23–0.71	170	124–217
	k ₄₅	1/h	0.2	0.09–0.31	–	–
	k ₄₀	1/h	0.5	0.33–0.77	48	35–62
Xanthine (CMT5)	k _{in5}	mg/L* ^a h	0.66	0.47–0.86	–	–
	E _{BASE} (5) ^b	mg/L	0.3 ^b	–	–	–
	Init _{5D}	mg/L	0.59	0.33–0.85	112 ^d	–
	k ₅₆	1/h	2.65	1.9–3.48	35	26–45
Uric acid (CMT6)	E _{BASE} (6) ^c	mg/L	25 ^c	–	–	–
	Init _{6D}	mg/L	37.98	30.57–45.1	37	27–48
	k ₆₀	1/h	0.032	0.026–0.039	34	27–43
Effect of disease severity	Moderate-severe HIE—Init _{4D}	–	2.9	1.59–4.35	–	–
	Moderate-severe HIE—Init _{5D}	–	1.2	0.69–2.04	–	–
<i>Residual variability</i>						
Allopurinol	Proportional error	%	29	24–36	–	–
	Additive error	mg/L	0.05 FIX	–	–	–
Oxypurinol	Additive error	mg/L	0.55	0.46–0.66	–	–
Hypoxanthine	Proportional error	%	53	45–63	–	–
Xanthine		%	35	30–41	–	–
Uric acid		%	14	12–17	–	–

CI confidence interval, *E_{BASE}(4)* hypoxanthine baseline value, *E_{BASE}(5)* xanthine baseline value, *E_{BASE}(6)* uric acid baseline value, *fm* formation fraction, *IC₅₀* half-maximal inhibitory concentration, *IIV* interindividual variability, *Init_{4D}* disease-related hypoxanthine initial value, *Init_{5D}* disease-related xanthine initial value, *Init_{6D}* disease-related uric acid initial value, *k₃₀* precursors clearance, *k₄₀* hypoxanthine salvage clearance, *k₄₅* hypoxanthine to xanthine clearance, *k₅₆* xanthine to uric acid clearance, *k₆₀* uric acid clearance, *k_{in4}* hypoxanthine synthesis rate, *k_{in5}* xanthine synthesis rate, *PD* pharmacodynamic, *PK* pharmacokinetic

$${}^a\text{E}_{\text{BASE}}(4) = \frac{k_{\text{in4}}}{k_{40} + k_{45}}$$

$${}^b\text{E}_{\text{BASE}}(5) = \frac{k_{\text{in5}} + (k_{45} * \text{E}_{\text{BASE}}(4))}{k_{56}}$$

$${}^c\text{E}_{\text{BASE}}(6) = \frac{k_{56} * \text{E}_{\text{BASE}}(5)}{k_{60}}$$

^dCorrelation of 1 was found between IIV in *Init_{4D}* and *Init_{5D}*. Therefore, the same ETA distribution was used. A scaling factor of 0.66 was estimated for IIV *Init_{5D}*

therefore, it was not included in the final model. As hypoxanthine and xanthine are derived from purine nucleotides inosine monophosphate and guanosine monophosphate, respectively, the strong correlation between IIV in *Init_{4D}* and *Init_{5D}* might indicate an impact of the hypoxic event.

3.4 Model Evaluation

The final model provided an adequate description for the data from both the allopurinol and mannitol groups. No substantial trend or bias was observed in the observed versus

population-predicted and individual-predicted concentration plots as well as the conditional weighted residual versus population-predicted concentration and time plots (Fig. 3). In the visual predictive check, no considerable misspecification was observed (Fig. 4).

4 Discussion

The metabolism of the purine bases hypoxanthine, xanthine, and uric acid in neonates with HIE was adequately described by this PK-PD model and the effect of allopurinol and oxypurinol on XOR inhibition was quantified. In this model, the degradation of hypoxanthine to xanthine and uric acid, the salvage of hypoxanthine, and the impact of precursor exhaustion on the synthesis of hypoxanthine and xanthine were implemented. Moreover, hypoxia-induced initial levels of hypoxanthine, xanthine, and uric acid were quantified, and were found to be higher in neonates classified as moderate-to-severe HIE cases compared with mild HIE cases.

The developed model was an extension of our published model based on neonates with HIE treated with allopurinol [16]. In the current study, data from neonates with HIE administered allopurinol and mannitol were analyzed, which allowed quantification of both disease-related and treatment-related PD effects. The pharmacokinetics of allopurinol and oxypurinol followed our previous study in neonates with HIE [16]. The redefined IC_{50} value of 0.68 mg/L for a combined allopurinol and oxypurinol concentration was slightly higher than our previous estimate of 0.36 mg/L [16]. Nevertheless, our previous statement that sufficient XOR inhibition was achieved with the dosing regimen applied in the ALBINO study should not be attenuated, as IC_{50} of 0.68 mg/L was still below all available observations in the first 72 hours of age. The low IC_{50} value confirmed that allopurinol and oxypurinol provided almost a full XOR inhibition during > 24 hours post-dose.

The effect of allopurinol on XOR inhibition can be further supported by the distinct xanthine concentration–time profile observed in the allopurinol and mannitol group, where

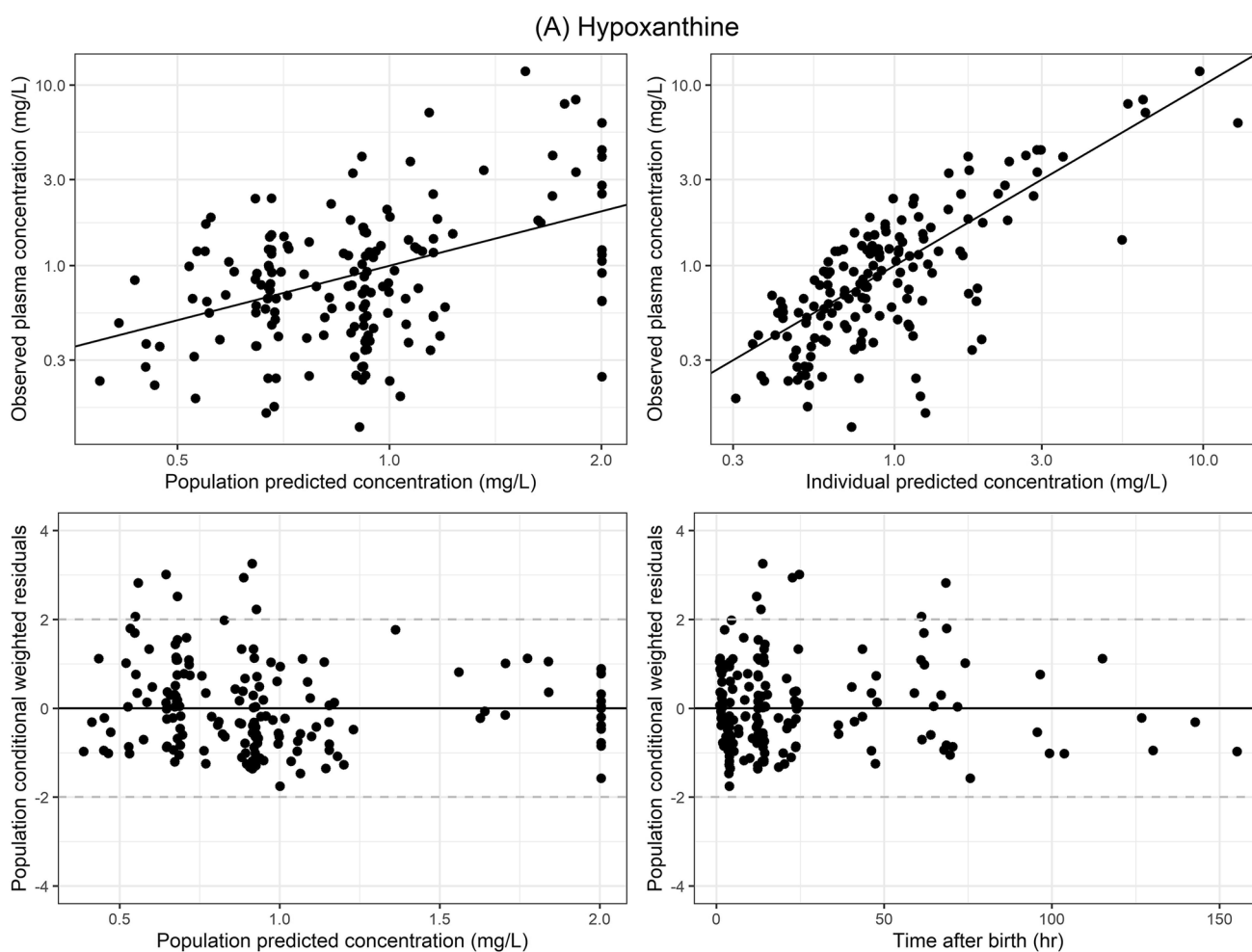


Fig. 3 Goodness of fit. *hr* hours

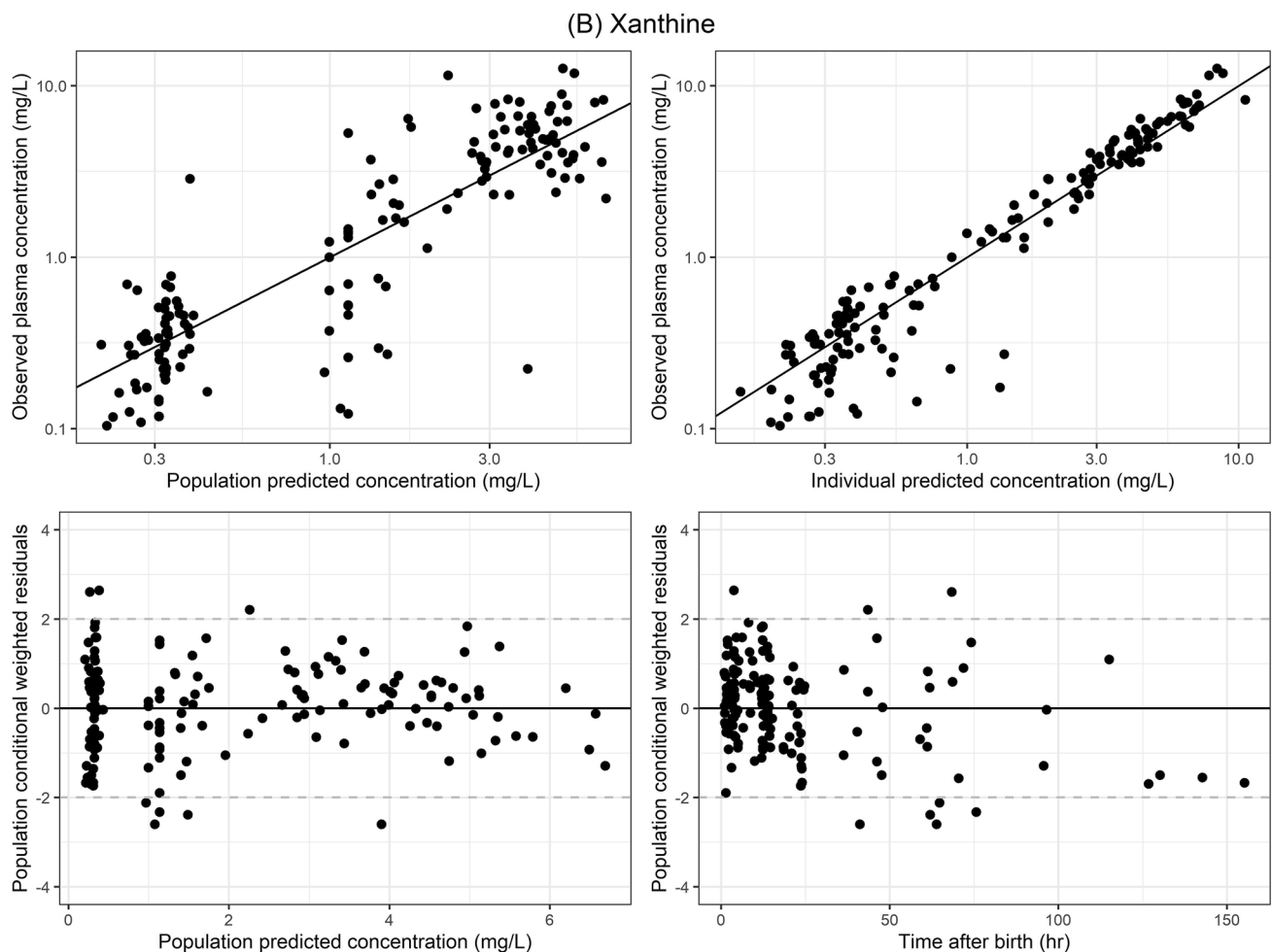


Fig. 3 (continued)

a surge in the xanthine level was seen in the allopurinol group only (Fig. 1). However, the two groups showed similar hypoxanthine and uric acid concentration–time profiles, which contrasted with the expectation of XOR inhibition (Fig. 1). This inconsistency was likely specific to asphyxiated neonates given the presence of disease-driven, high initial purine base levels. The rapid decline in the hypoxanthine level followed our previous assumption that the observed concentration profile represented the elimination of hypoxia-induced hypoxanthine, and masked the accumulation of hypoxanthine attributable to enzyme inhibition [31]. For uric acid, it was expected that XOR inhibition by allopurinol would lead to a faster drop in uric acid concentration; however, a similar clearance was observed in both the allopurinol and placebo groups. Uric acid is the end product of the complicated purine metabolism, therefore, the observations in the relatively short study period may mainly reflect the excretion of excessive uric acid driven by hypoxia.

Under normal conditions, it is estimated that 90% of hypoxanthine generated is salvaged rather than degraded or

excreted [2]. During hypoxia, salvaging is hindered because of energy deficiency and oxygen deprivation [4, 5]. In this analysis, the salvage pathway accounted for 68% of total hypoxanthine clearance in neonates, suggesting a consequence of extreme accumulation of hypoxanthine in HIE. However, in neonates given allopurinol, hypoxanthine salvage enhanced to 75%, showing the advantage of allopurinol in HIE. The greater salvage is known to result in the accumulation of adenosine, which is a central nervous system neuromodulator that provides additional neuroprotection [32]. Therefore, the higher hypoxanthine salvage in the allopurinol treatment group as identified in this study might strengthen the beneficial role of allopurinol in improving neurological outcomes in neonates with HIE.

The high initial levels of hypoxanthine, xanthine, and uric acid estimated revealed an impact of hypoxia. Using hypoxanthine and uric acid levels as biomarkers for HIE severity prediction has been highlighted in several studies [6, 12–15]. In this study, neonates with moderate-to-severe HIE exhibited 2.9-fold and 1.2-fold, respectively higher

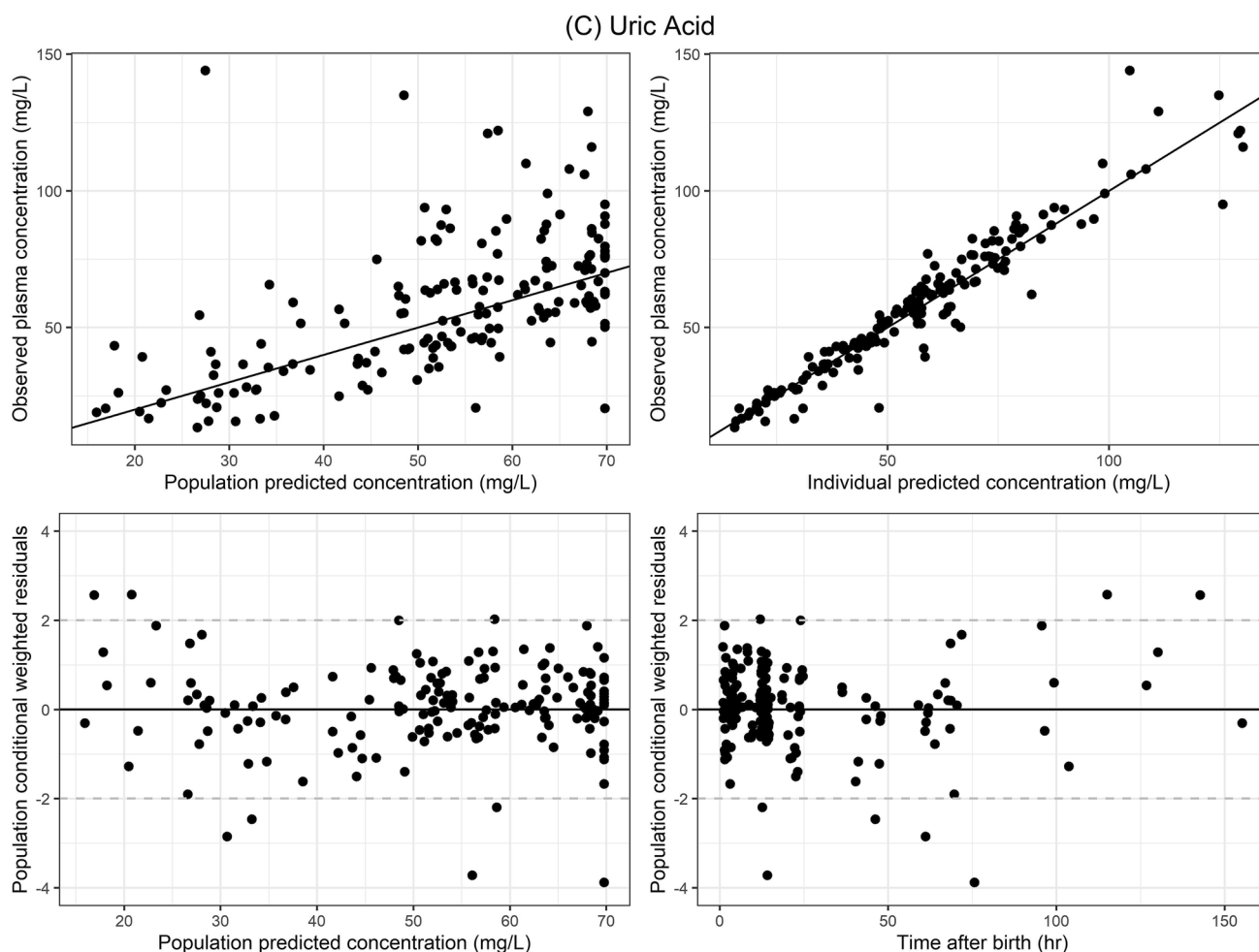


Fig. 3 (continued)

disease-related initial hypoxanthine and xanthine levels compared with neonates with mild HIE. In addition, higher disease-related initial hypoxanthine, xanthine, and uric acid estimates in neonates with a Thompson score ≥ 8 and with very high LDH and ALT values were demonstrated in graphical analyses (Figs. 1, 2 of the Electronic Supplementary Material [ESM]). A 100% correlation was found between IIV in disease-related hypoxanthine and xanthine levels. This strong correlation followed the pathophysiology of hypoxia, as an AMP breakdown increases levels of purine nucleotides inosine monophosphate and guanosine monophosphate and results in high hypoxanthine and xanthine exposures, respectively.

To improve the description of hypoxanthine and xanthine endogenous turnover, an empirical precursor compartment was added in our model and a net decrease in precursor amount was assumed. The decrease in precursor amount subsequently reduced the synthesis of hypoxanthine and xanthine by 0.43% per hour and improved the model goodness of fit. Previous studies *in vitro* and *in vivo* found a

rapid decline in purine nucleotides and nucleosides following a hypoxic event, which supports our hypothesis [28, 29]. Although xanthine concentrations after 24 hours post-dose were not fully captured, the decreasing hypoxanthine and xanthine synthesis identified in our model underlined the effect of precursor exhaustion on the dynamics of hypoxanthine and xanthine in neonates with HIE.

Investigating the impact of TH on drug clearance and potential biomarker dynamics has been a topic of interest. It is known that TH decreases heart rate and cardiac output. Consequently, this reduces kidney and liver perfusion [24]. In addition, TH protracts enzymatic reactions, which further reduces free radical production [33]. Unfortunately, the effect of TH cannot be distinguished from the severity of hypoxia in our study because the neonates classified as moderate-to-severe HIE all underwent TH treatment. Neonates experiencing more severe HIE often experience more hypoxia, leading to more attenuated organ function; therefore, the impact of TH on PK-PD parameters could not be elucidated. In the study of Róka et al., factors reflecting

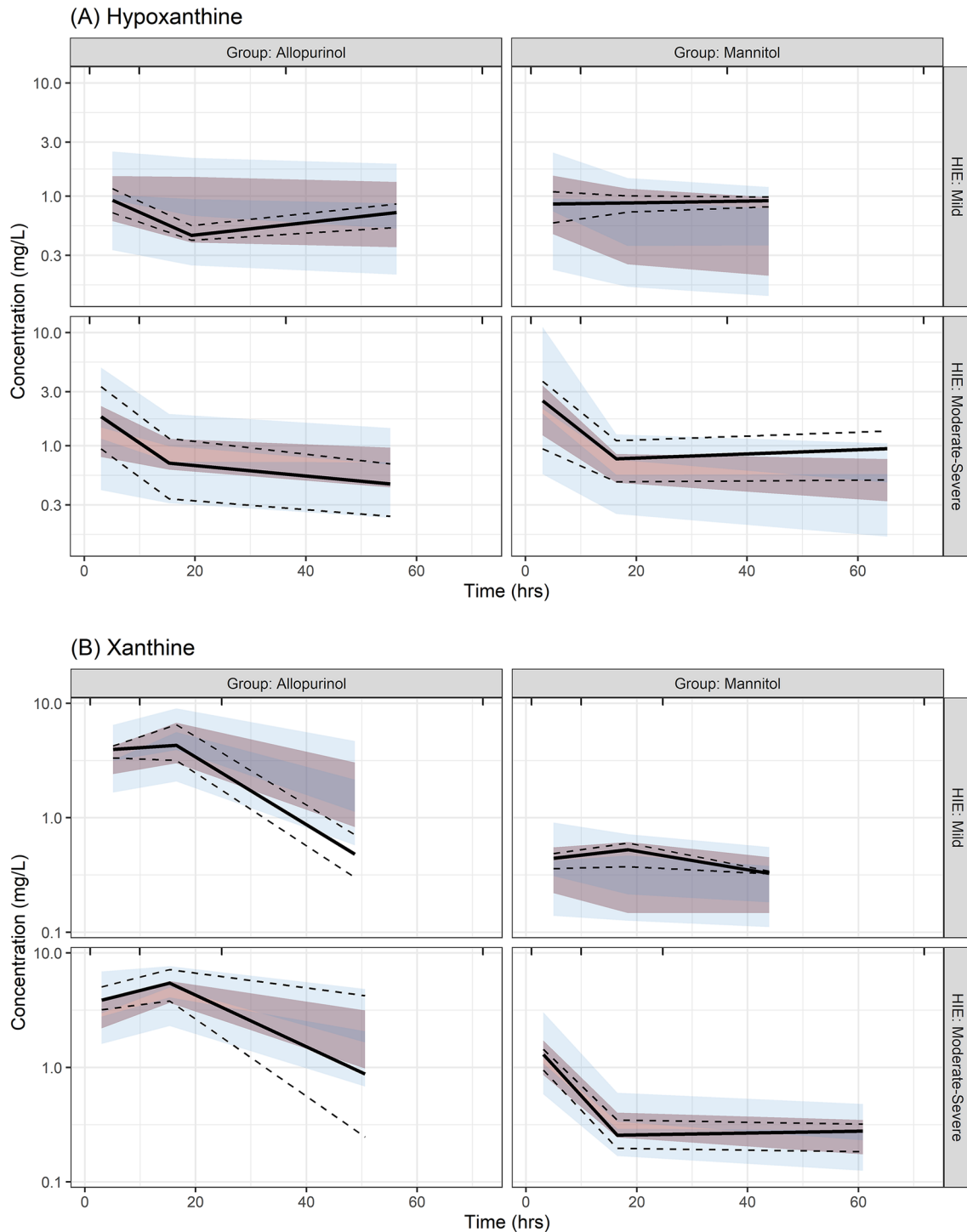


Fig. 4 Visual predictive checks. *HIE* hypoxic-ischemic encephalopathy, *hrs* hours

cell necrosis and tissue damage including ALT, LDH, and uric acid were lower in neonates with moderate-to-severe HIE treated with TH compared with neonates receiving no TH treatment, supporting the advantage of TH in HIE [13]. In the study of Deferm et al., mannitol clearance in

TH-treated patients decreased by 60%, indicating an alteration in the glomerular filtration rate [17]. However, the study was based on data from the ALBINO placebo cohort; therefore, interpreting the result could be confounded by disease severity.

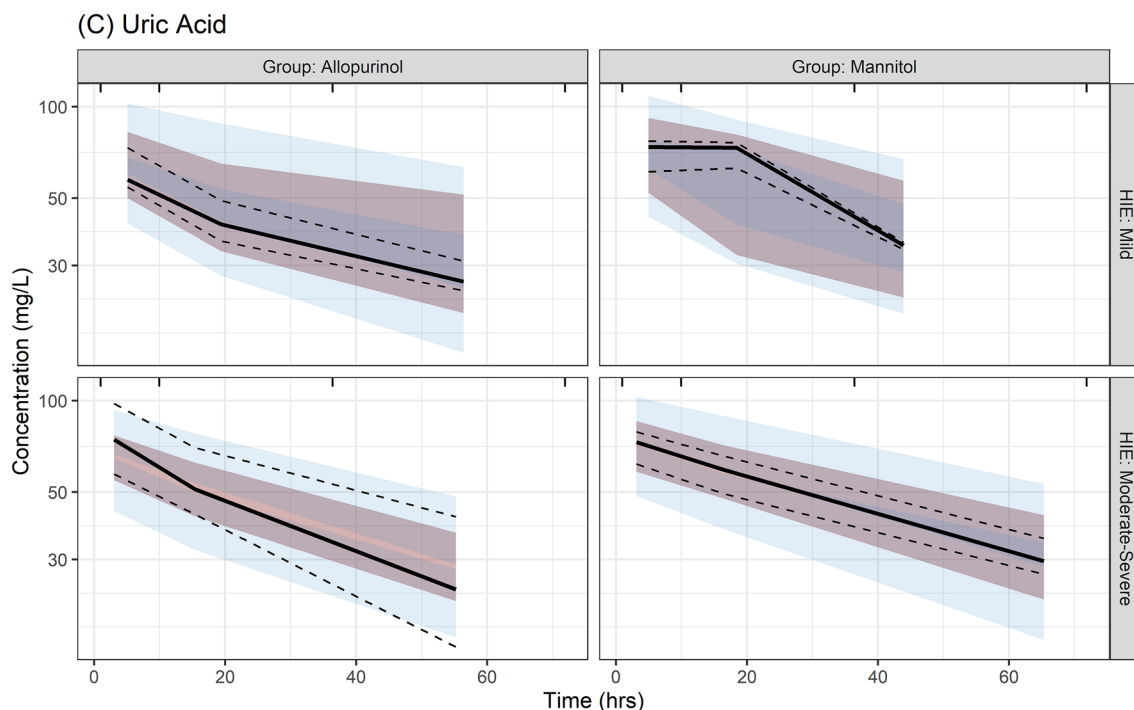


Fig. 4 (continued)

5 Conclusions

This extended PK-PD model provided an adequate description of the complex hypoxanthine, xanthine, and uric acid metabolism in asphyxiated neonates treated with allopurinol. A low IC_{50} on XOR inhibition and a high fraction of hypoxanthine salvage were quantified, indicating a positive pharmacological effect of allopurinol treatment. The impact of hypoxia on hypoxanthine, xanthine, and uric acid dynamics was characterized in the model, suggesting higher hypoxia-related initial hypoxanthine and xanthine values with a more severe HIE status and a declining rate of hypoxanthine and xanthine synthesis as a consequence of exhausting purine precursors. The developed model provides new insights into the evaluation of the efficacy of allopurinol and the investigation of suitable biomarker in neonates with HIE.

Supplementary Information The online version contains supplementary material available at <https://doi.org/10.1007/s40262-022-01164-9>.

Acknowledgements The ALBINO Study Group involved in this project consists of the coordinating investigators, the pharmacokinetic study group, and the beneficiaries and national coordinators. Coordinating investigators are Axel R. Franz (University Hospital Tuebingen, Tuebingen, Germany) and Mario Rüdiger (University Hospital CG Carus, Medizinische Fakultät der TU Dresden, Dresden, Germany). The contributors to the pharmacokinetic study group are Laura Nijstad and Kim Annink (Utrecht, the Netherlands), Christian Maiwald (Tuebingen, Germany), Michael Schroth and Anja Hagen (Nuremberg, Germany) and Loubna el Bakkali and Mirjam M. van Weisenbruch

(Amsterdam, the Netherlands). The beneficiaries and national coordinators are Axel R. Franz and Christian F. Poets (Tuebingen, Germany), Mario Rüdiger (Dresden, Germany), Manon Benders and Frank van Bel (Utrecht, the Netherlands), Karel Allegaert and Gunnar Nauelaers (Leuven, Belgium), Dirk Bassler (Zurich, Switzerland), Katrin Klebermass-Schrehof (Vienna, Austria), Maximo Vento (Valencia, Spain), Hercilia Guimaraes (Porto, Portugal), Tom Stiris (Oslo, Norway), Isabella Mauro (Udine, Italy), Marjo Metsäranta (Helsinki, Finland), Sampsä Vanhatalo (Helsinki, Finland), Jan Mazela (Poznan, Poland), Tuuli Metsvaht (Tartu, Estonia), and Roselinda van der Vlugt-Meijer (ACE Pharmaceuticals, Zeewolde, the Netherlands).

Declarations

Funding The ALBINO study is funded under the Horizon 2020 Framework EU Program call H2020-PHC-2015-two-stage grant 667224. The research on the pharmacokinetics during whole body hypothermia (KA) is further supported by the iPREDICT project (FWO Senior research project, fundamental research, GOD0520N).

Conflict of interest All authors have no conflicts of interest to declare.

Ethics approval The data used in this study were acquired in accordance with the Declaration of Helsinki and the guidelines of Good Clinical Practice. The ALBINO study was granted by institutional review boards and independent ethics committees. The Medical Ethics Committee of the University Medical Centre Utrecht and the Central Committee on Human Research approved the study including the specific pharmacokinetic sub-study for the Netherlands (NL57237.041.16). The German Federal Authority (EudraCT 2016-000222-19) as well as the leading Ethics Committee of Tübingen approved the study for Germany.

Consent to participate Short oral consent was obtained from at least one parent before administering the study medication. After the first dose, but before the (potential) second dose, full written parental consent was obtained. In the case where parents did not sign the informed consent, blood samples already collected shortly after birth were destroyed.

Availability of data and material The raw data are available upon reasonable request by an e-mail to the corresponding author, while blinding for group allocation should be respected until the primary outcome analysis has been finalized.

Code availability Not applicable.

Authors' contributions KA and the ALBINO study group were responsible for protocol development, study conduct, study registration, study recruitment, and data collection. Population pharmacokinetic-pharmacodynamic modeling was performed by WC, TD, and AH. The draft of the manuscript was written and reviewed by WC, KA, TD, and AH. All authors and contributors have read and commented on the manuscript and have approved the submitted version.

Open Access This article is licensed under a Creative Commons Attribution-NonCommercial 4.0 International License, which permits any non-commercial use, sharing, adaptation, distribution and reproduction in any medium or format, as long as you give appropriate credit to the original author(s) and the source, provide a link to the Creative Commons licence, and indicate if changes were made. The images or other third party material in this article are included in the article's Creative Commons licence, unless indicated otherwise in a credit line to the material. If material is not included in the article's Creative Commons licence and your intended use is not permitted by statutory regulation or exceeds the permitted use, you will need to obtain permission directly from the copyright holder. To view a copy of this licence, visit <http://creativecommons.org/licenses/by-nc/4.0/>.

References

- Allen KA, Brandon DH. Hypoxic ischemic encephalopathy: pathophysiology and experimental treatments. *Newborn Infant Nurs Rev.* 2011;11:125–33.
- Jiménez RT, Puig JG. Purine metabolism in the pathogenesis of hyperuricemia and inborn errors of purine metabolism associated with disease. In: Robert Terkeltaub, Gout and other crystal arthropathies. W.B. Saunders Philadelphia; 2012. pp. 36–50. <https://doi.org/10.1016/B978-1-4377-2864-4.10003-X>, <https://www.sciencedirect.com/science/article/pii/B978143772864410003X>
- Wheaton WW, Chandel NS. Hypoxia. 2. Hypoxia regulates cellular metabolism. *Am J Physiol Cell Physiol.* 2011;300:C385–93.
- Ichida K, Hosoyamada M, Hosoya T, Endou H. Primary metabolic and renal hyperuricemia. *Genet Dis Kidney.* Academic Press, Richard P. Lifton and Stefan Somlo and Gerhard H. Giebisch and Donald W. Seldin, Kimiyoshi Ichida and Makoto Hosoyamada and Tatsuo Hosoya and Hitoshi Endou, San Diego 2009;651–60. 978-0 12-449851-8, <https://doi.org/10.1016/B978-0-12-449851-8.00038-3>, <https://www.sciencedirect.com/science/article/pii/B9780124498518000383>.
- Murray AW. The biological significance of purine salvage. *Annu Rev Biochem.* 1971;40:811–26. <https://doi.org/10.1146/annurev.bi.40.070171.004115>
- Saugstad OD. Hypoxanthine as an indicator of hypoxia: Its role in health and disease through free radical production. *Pediatr Res.* 1988;23:143–50.
- Saugstad OD, Oei JL, Lakshminrusimha S, Vento M. Oxygen therapy of the newborn from molecular understanding to clinical practice. *Pediatr Res.* 2019;85:20–9.
- Liu L, Oza S, Hogan D, Chu Y, Perin J, Zhu J, et al. Global, regional, and national causes of under-5 mortality in 2000–15: an updated systematic analysis with implications for the sustainable development goals. *Lancet.* 2016;388:3027–35.
- Annink KV, Franz AR, Derks JB, Rüdiger M, van Bel F, Benders MJNL. Allopurinol: old drug, new indication in neonates? *Curr Pharm Des.* 2018;23:5935–42.
- Maiwald CA, Annink KV, Rüdiger M, Benders MJNL, Van Bel F, Allegaert K, et al. Effect of allopurinol in addition to hypothermia treatment in neonates for hypoxic-ischemic brain injury on neurocognitive outcome (ALBINO): study protocol of a blinded randomized placebo-controlled parallel group multicenter trial for superiority phase. *BMC Pediatr.* 2019;19:210.
- Day RO, Graham GG, Hicks M, McLachlan AJ, Stocker SL, Williams KM. Clinical pharmacokinetics and pharmacodynamics of allopurinol and oxypurinol. *Clin Pharmacokinet.* 2007;46:623–44.
- Saugstad OD. Hypoxanthine as a measurement of hypoxia. *Pediatr Res.* 1975;9:158–61.
- Róka A, Vásárhelyi B, Bodrogi E, Machay T, Szabó M. Changes in laboratory parameters indicating cell necrosis and organ dysfunction in asphyxiated neonates on moderate systemic hypothermia. *Acta Paediatr.* 2007;96:1118–21.
- Beken S, Aydın B, Dilli D, Erol S, Zenciroğlu A, Okumuş N. Can biochemical markers predict the severity of hypoxic-ischemic encephalopathy? *Turk J Pediatr.* 2014;56:62–8.
- Patel KP. Urinary uric acid/creatinine ratio: a marker for perinatal asphyxia. *J Clin Diagn Res.* 2017;11:SC08–10.
- Chu W-Y, Annink KV, Nijstad AL, Maiwald CA, Schroth M, El Bakkali L, et al. Pharmacokinetic/pharmacodynamic modelling of allopurinol, its active metabolite oxypurinol, and biomarkers hypoxanthine, xanthine and uric acid in hypoxic-ischemic encephalopathy neonates. *Clin Pharmacokinet.* 2022;61:321–33.
- Deferm N, Annink KV, Faelens R, Schroth M, Maiwald CA, el Bakkali L, et al. Glomerular filtration rate in asphyxiated neonates under therapeutic whole-body hypothermia, quantified by mannitol clearance. *Clin Pharmacokinet.* 2021;60:897–906.
- Beal S, Sheiner L, Boeckmann A, Bauer R. NONMEM users guides. ICON Development Solutions, Gaithersburg, Maryland; 2013.
- Lindbom L, Ribbing J, Jonsson EN. Perl-speaks-NONMEM (PsN): a Perl module for NONMEM related programming. *Comput Methods Programs Biomed.* 2004;75:85–94.
- Keizer RJ, van Bentem M, Beijnen JH, Schellens JHM, Huitema ADR, Piraña and PCluster: a modeling environment and cluster infrastructure for NONMEM. *Comput Methods Programs Biomed.* 2011;101:72–9.
- Thompson CM, Puterman AS, Linley LL, Hann FM, Van Der Elst CW, Moltano CD, et al. The value of a scoring system for hypoxic ischaemic encephalopathy in predicting neurodevelopmental outcome. *Acta Paediatr.* 1997;86:757–61.
- Ebert EC. Hypoxic liver injury. *Mayo Clin Proc.* 2006;81:1232–6.
- Karlsson M, Wiberg-Itzel E, Chakkarapani E, Blennow M, Winblad B, Thoresen M. Lactate dehydrogenase predicts hypoxic ischaemic encephalopathy in newborn infants: a preliminary study. *Acta Paediatr.* 2010;99:1139–44.
- Sehgal A, Linduska N, Huynh C. Cardiac adaptation in asphyxiated infants treated with therapeutic hypothermia. *J Neonatal Perinatal Med.* 2019;12:117–25.

25. Bergstrand M, Hooker AC, Wallin JE, Karlsson MO. Prediction-corrected visual predictive checks for diagnosing nonlinear mixed-effects models. *AAPS J*. 2011;13:143.
26. Dosne AG, Bergstrand M, Karlsson MO. An automated sampling importance resampling procedure for estimating parameter uncertainty. *J Pharmacokinet Pharmacodyn*. 2017;44:509–20.
27. Fox IH. Metabolic basis for disorders of purine nucleotide degradation. *Metabolism*. 1981;30:616–34.
28. Hagberg H, Andersson P, Lacarewicz J, Jacobson I, Butcher S, Sandberg M. Extracellular adenosine, inosine, hypoxanthine, and xanthine in relation to tissue nucleotides and purines in rat striatum during transient ischemia. *J Neurochem*. 1987;49:227–31.
29. del Castillo V-M, Hernández-Camacho CJ, Méndez-Rodríguez LC, Zenteno-Savín T. Purine metabolism in response to hypoxic conditions associated with breath-hold diving and exercise in erythrocytes and plasma from bottlenose dolphins (*Tursiops truncatus*). *Comp Biochem Physiol A Mol Integr Physiol*. 2016;191:196–201.
30. Fisher O, Benson RA, Imray CH. The clinical application of purine nucleosides as biomarkers of tissue ischemia and hypoxia in humans in vivo. *Biomark Med*. 2019;13(11):953–65.
31. Marro PJ, Baumgart S, Delivoria-Papadopoulos M, Zirin S, Corcoran L, McGaurn SP, et al. Purine metabolism and inhibition of xanthine oxidase in severely hypoxic neonates going onto extracorporeal membrane oxygenation. *Pediatr Res*. 1997;41:513–20.
32. Marro PJ, Mishra OP, Delivoria-Papadopoulos M. Effect of allopurinol on brain adenosine levels during hypoxia in newborn piglets. *Brain Res*. 2006;1073–1074:444–50.
33. Si QS, Nakamura Y, Kataoka K. Hypothermic suppression of microglial activation in culture: inhibition of cell proliferation and production of nitric oxide and superoxide. *Neuroscience*. 1997;81:223–9.

Authors and Affiliations

Wan-Yu Chu¹ · Karel Allegaert^{2,3} · Thomas P. C. Dorlo¹ · Alwin D. R. Huitema^{1,4,5} on behalf of the ALBINO Study Group

¹ Department of Pharmacy and Pharmacology, Netherlands Cancer Institute, Amsterdam, The Netherlands

² Department of Development and Regeneration, and Department of Pharmaceutical and Pharmacological Sciences, Leuven, Belgium

³ Department of Clinical Pharmacy, Erasmus MC, Rotterdam, The Netherlands

⁴ Department of Pharmacology, Princess Máxima Center for Pediatric Oncology, Utrecht, The Netherlands

⁵ Department of Clinical Pharmacy, University Medical Center Utrecht, Utrecht University, Utrecht, The Netherlands